Coastal groundwater level trends reveal global susceptibility to seawater intrusion

Annika Nolte[1,2*], Steffen Bender[1], Jens Hartmann[2], Stefan Baltruschat[1,2], Nils Moosdorf[3,4], Robert Reinecke[5]

[1]Climate Service Center Germany (GERICS), Helmholtz-Zentrum Hereon, Hamburg, Germany

[2]Institute for Geology, Center for Earth System Research and Sustainability, Universität Hamburg, Hamburg, Germany

[3]Leibniz Centre for Tropical Marine Research (ZMT), Bremen, Germany

[4]Institute of Geosciences, Kiel University, Kiel, Germany

[5]Institute of Geography, Johannes Gutenberg University Mainz, Mainz, Germany

*****Corresponding author

Abstract

Coastal groundwater is a vital source of freshwater that is threatened by overabstraction and rising sea levels. Yet, our understanding of where global coastal groundwater levels (GWLs) are declining and what regions are susceptible to future seawater intrusion (SWI) remains limited. Here, we present the first global, observation-based assessment of coastal GWL trends, using more than 550,000 in-situ well records. From 1990 to 2024, 21% of coastal wells had significant GWL trends (±0.1 m year^{-1}), rising to 28% in the last 9 years, when declines became more frequent. More pronounced changes are observed in deeper (s_rho=0.61), arid (s_rho=0.53), and rural wells (s_rho=0.23). Because declining GWLs weaken freshwater-seawater gradients that resist SWI, we identify susceptible coastal hotspots with stabilizing (3.7%), persistent (92.0%), and emerging (4.3%) conditions, with emerging hotspots in Australia, Europe, West India, and North America. Our findings emphasize the need to understand SWI intrusion across coastal landscapes to ensure safe drinking water for coastal communities.

Introduction

Groundwater is a critical freshwater source in coastal regions, which are home to 2.86 billion people (Cosby *et al* 2024), and plays a vital role in sustaining coastal ecosystems (Dyring *et al* 2022). However, coastal aquifers face pressure from growing coastal populations (Neumann *et al* 2015), and are increasingly vulnerable to seawater intrusion (SWI), which threatens both the quantity and quality of available water. Climate change and, as a consequence, sea-level rise, changes in groundwater recharge, and intensifying water use (IPCC 2021, Spinoni *et al* 2021) increase pressure on coastal groundwater systems, especially in low-lying coastal areas with limited topographic relief or in arid regions where natural groundwater recharge is limited (Ferguson and Gleeson 2012, Michael *et al* 2013, Richardson *et al* 2024). These hydroclimatic conditions make aquifers in coastal settings susceptible to SWI, particularly when already accompanied by declining groundwater levels (GWLs). This study aims to identify where such SWI-susceptible conditions are already present and where emerging risks under climate change may be especially critical to monitor.

In-situ observations of GWLs provide insights into the susceptibility of coastal aquifer systems to SWI (Jasechko *et al* 2020, Renu *et al* 2025): flat land-sea hydraulic gradients indicate limited buffering capacity, while declining GWLs are a driver of reduced freshwater outflow that can destabilize the freshwater-saltwater interface, propagate it inland, and lead to long-term degradation of aquifer systems (Ferguson and Gleeson 2012, Jasechko *et al* 2020, Kretschmer *et al* 2025a, Renu *et al* 2025). Depth to groundwater (i.e., water table depth, WTD) plays a key role in modulating this vulnerability: in topography-limited systems,

low elevation and small hydraulic gradients mean that even modest GWL declines can substantially reduce seaward flow (Michael *et al* 2013). This susceptibility is further exacerbated in arid and semi-arid settings, where natural groundwater recharge is already limited. Recharge is particularly sensitive to climate variability when potential evapotranspiration only slightly exceeds precipitation (Berghuijs *et al* 2024), whereas GWLs tend to be more sensitive to changes in water balance in arid regions, where long groundwater response times allow climate-driven changes to exert a strong but slower influence (Cuthbert *et al* 2019b, Fan *et al* 2023). In many arid coastal areas, climate change is expected to intensify groundwater stress and salinization risks by further reducing recharge through increasing aridity and shifts in precipitation patterns (Richardson *et al* 2024).

Yet despite our current process understanding, the global spatiotemporal distribution of SWI-susceptible conditions according to this understanding remains poorly characterized. This limits our ability to anticipate where and how salinization pressures may intensify under future climatic and anthropogenic change and reflects broader limitations in global groundwater assessments, which often lack the resolution, integration, and observational grounding needed to capture the complexity of coastal systems (Gleeson *et al* 2020). Most assessments of coastal groundwater systems are focused in local or regional case studies (e.g., Morgan and Werner 2015; Costall *et al* 2020), which limits the results to a specific area and scale and presents challenges of commensurability when seeking a better understanding of global-scale processes (Gleeson *et al* 2021). Global modeling approaches (e.g., Adams *et al* 2024, Zamrsky *et al* 2024) continue to face high uncertainties, are challenging to evaluate due to the limited, spatially-biased availability of time-varying GWL data (Gleeson *et al* 2021, Reinecke *et al* 2024), and are only beginning to incorporate density-driven processes critical for assessing SWI (Kretschmer *et al* 2025a). GRACE (Gravity Recovery and Climate Experiment) satellite observations provide valuable information for major groundwater basins, but their coarse spatial resolution and reliance on model-based separation of water components limit their applicability, especially in smaller or coastal systems (Frappart and Ramillien 2018, Costantini *et al* 2023).

In contrast, in-situ GWL observations offer key indicators of coastal groundwater susceptibility to SWI, such as landward gradients and declining levels, but remain difficult to integrate at scale due to fragmented responsibilities, limited digitization, accessibility issues, and non-standardized datasets (Famiglietti and Rodell 2013, Lall *et al* 2020, United Nations 2022). Despite these challenges, few efforts have leveraged large-sample in-situ GWL data. Fan *et al* (2013) were the first to compile GWL observations globally. This was the basis for developing modeled estimates of WTD to achieve global coverage (e.g., Fan *et al* 2013, Ma *et al* 2024), now widely used in groundwater-related environmental studies (e.g., Shokri-Kuehni *et al* 2020). Jasechko *et al* (2024) and Chávez García Silva *et al* (2024) assessed GWL trends at broad scales, though coastal regions remained underrepresented. By contrast, Jasechko *et al* (2020) focused on coastal

areas but limited their analysis to the contiguous United States. Collectively, these studies underscore both the value of in-situ GWL data and the persistent gap in globally integrated, observationally grounded assessments of coastal aquifers. To address this gap, we compiled existing global in-situ GWL observations to assess spatiotemporal patterns in coastal groundwater systems and linked these observational signals to aridity, coastal proximity, and population density. Specifically, we investigated where hydroclimatic conditions indicative of SWI susceptibility occur, and how these settings are associated with GWL changes.

Susceptible hydroclimatic conditions

Hydroclimatic conditions that increase the susceptibility to SWI – flat hydraulic gradients, shallow GWLs, and arid climates – are widespread in global coastal zones, especially near the coastline, but also extend further inland. Globally, GWLs near coasts are often shallow: the median coastal WTD is 6.1 m, and nearly half of all observations are shallower than 5 m (Supplement A). WTD adds susceptibility context because shallow tables can coincide with small freshwater head and limited vadose storage; we therefore assess buffer capacity via the land–sea hydraulic gradient. Flat hydraulic gradients, which weaken the natural flow of groundwater toward the sea, are found in about one-third of all observed coastal areas. Although steeper gradients dominate overall (skewed distribution in Fig. 1A), flat gradients remain common even tens of kilometers inland (34-37% of all observations; Fig. 1C). Compared to the global aridity distribution of coastal regions, our dataset shows a distinct clustering near the transitional AI value of approximately 1 (marking the boundary between water- and energy-limited climates). In contrast, moderately arid regions ($AI \approx 0.3–0.7$) and humid regions ($AI \gg 1$) are underrepresented (Fig. 1B). Overall, 74% of observations fall within water-limited environments ($AI \leq 1$).

When flat gradients and arid climates co-occur, they form the most susceptible cluster (C1). These conditions are most frequently observed within 1 km of the coastline (28 % of observations), but also persist inland (Fig. 1C). The clearest and most continuous C1 patterns appear in regions such as the southeastern U.S., Gulf of Mexico, and northeast Australia, regions where data density is high enough to support this identification (Fig. 1D). Steep-gradient, water-limited settings (C2) are the most common across all coastal distances, comprising 52% of near-coastal observations. In contrast, C3 conditions, where gradients are low but recharge is not limited, represent the least common susceptibility configuration.

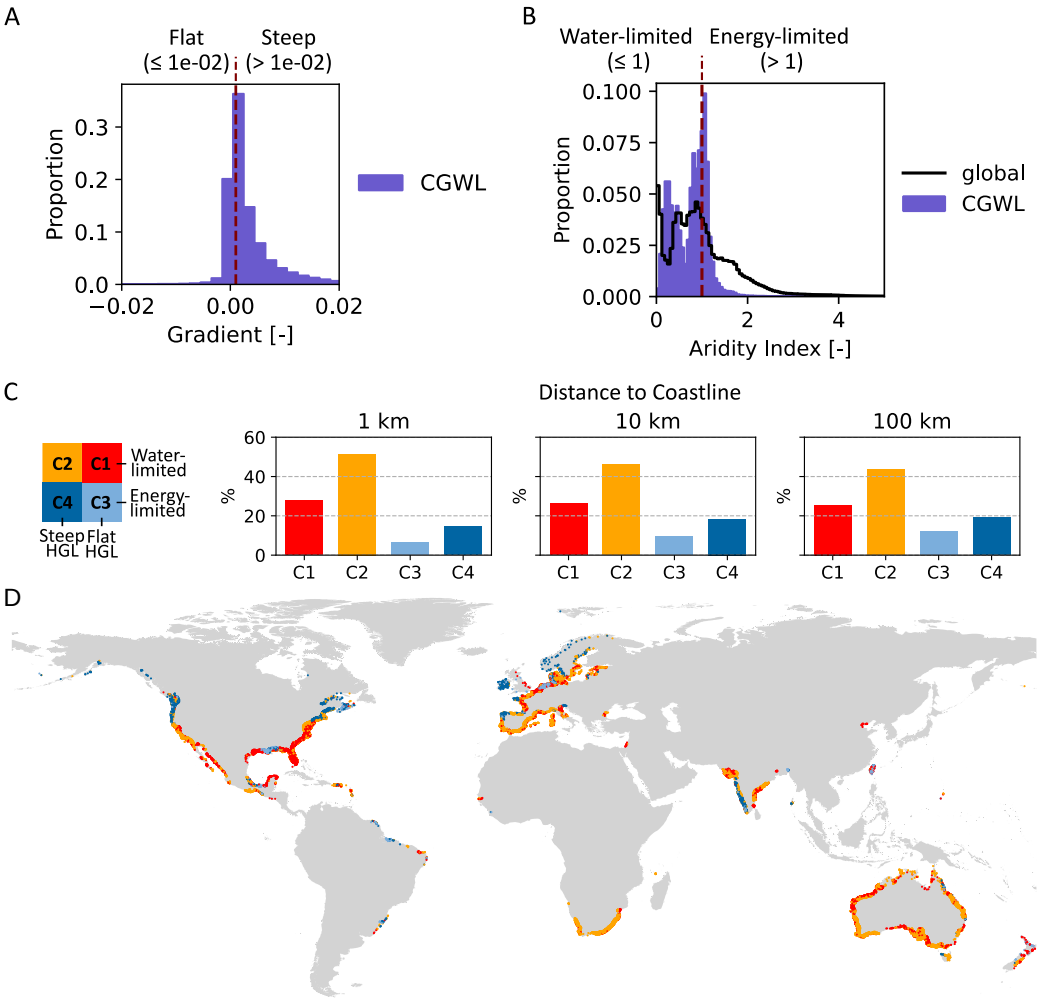

Fig. 1 Global patterns of hydroclimatic conditions indicating susceptibility of coastal groundwater systems to seawater intrusion. (A) Distribution of hydraulic gradients derived from the CGWL dataset, with a red dashed line marking the threshold separating flat ($\leq 10^{-2}$) and steep conditions. (B) Distribution of aridity index (AI) values for the CGWL dataset and global coastal regions, with a red dashed line marking the climatic threshold (AI ≈ 1) used to distinguish water- and energy-limited regimes. (C) Proportions of four hydroclimatic susceptibility clusters (C1–C4) at three distances from the coastline (1 km, 10 km, 100 km). (D) Global distribution of individual categorized observations (plotted in grid cell centers with random overlap of clusters).

Trends in rural and urban coastal regions

Trends of GWL changes are more pronounced in rural than in urban coastal regions. Over the 9-year period, 28% of observations show statistically significant GWL changes within the last 34 years (1990-2024) of at least ±0.1 m per year, compared to 21% over the 19-year period. The frequency of upward and downward changes in GWLs is relatively balanced across both periods, with a slight bias toward declines in the shorter timeframe (12% increase, 16% decrease). Most observations (over 80%) exhibit consistent change direction across both periods.

GWL changes within 9-year periods are displayed with their regional frequency, magnitude, and direction in Fig. 2. The prevalence of both declining and rising GWLs varies spatially, ranging from under 10% (e.g., northern Europe) to over 50% (e.g., South Africa and the Gulf of Mexico). While Fig. 2 summarizes regional GWL trends across IPCC subregions, substantial variation is evident within individual regions, as shown by the individual observations on the map. These display diverse magnitudes and directions of change, often occurring in spatially clustered patterns within the same region.

Furthermore, Fig. 2 reveals a consistent pattern of rural–urban (Eurostat 2021) differences in GWL changes. Across both assessment periods, rural areas show a higher prevalence of significant GWL trends than urban areas. The trend magnitude is negatively correlated with population density in 2020 (Spearman's rank correlation coefficient (s_rho) = -0.23). Over the 9-year period, 30% of rural observations exhibit significant upward and downward trends, compared to 25% in urban areas. Similarly, over the 19-year period, 23% of rural sites show trends versus 18% in urban areas. This global pattern is mirrored in several regions. For instance, in India, southeastern Australia, western North America, and the Mediterranean.

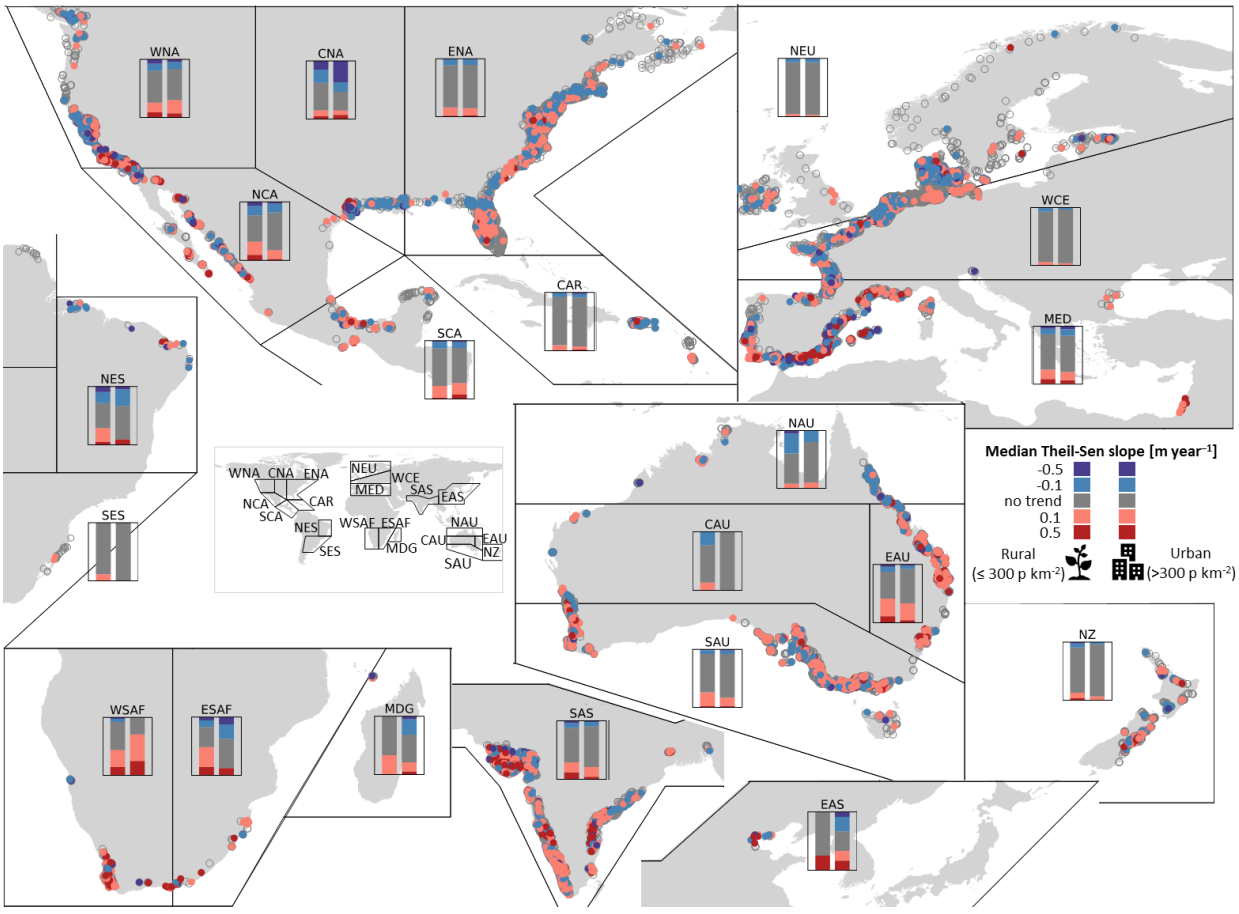

Fig. 2 Spatial patterns of recent 9-year groundwater level trends across global coastal zones, grouped by IPCC subregions (Iturbide *et al* 2020). Colored points on maps represent individual trend observations that are plotted in grid cell centers with random overlap of Theil-Sen slope trend categories on top of "no trend":

strong decline (< –0.5 m year^{-1}, dark blue), moderate decline (–0.5 to –0.1 m year^{-1}, light blue), no trend (–0.1 to 0.1 m/yr and/or non-significant, gray), moderate rise (0.1 to 0.5 m year^{-1}, light red), and strong rise (> 0.5 m year^{-1}, dark red). Bar charts show the proportion of trend categories per region (≥ 10 observations), stratified by rural (≤300 people km^{-2}) and urban (>300 people km^{-2}) areas (CIESIN 2018). Supporting trend results are provided in Supplement B-3.

Identifying hotspots of seawater intrusion susceptibility

Hotspots of possible future sustainability to SWI can be identified for all continents. At 100 km from the coast, strong relationships emerge between the 9- and 19-year annual changes in GWLs (regardless of direction) and site characteristics. The trend magnitude over 19 years is correlated with aridity (s_rho = 0.53), WTD (s_rho = 0.61), and hydraulic gradient (s_rho = -0.25). At 1 km from the coast, these correlations weaken substantially but still exist (s_rho = 0.19 for aridity; s_rho = 0.45 for WTD; s_rho = -0.19 for gradient).

These relationships are also reflected in the distribution of GWL trends across the four susceptibility clusters (Fig. 3A). Water-limited clusters (C1 and C2) have the highest frequency of both upward and downward trends across all coastal distances and both periods. Near the coast, the co-occurrence of largest susceptibility and long-term GWL changes peaks: within 1 km, 31% of C1 observations show trends over the 19-year period – slightly more of them downward than upward. Steep-gradient clusters (C2 and C4) show notably higher percentages of GWL trends in the recent 9-year period compared to the 19-year baseline, with increases up to 12–14 percentage points in some distance bins. Further inland (100 km) and under water-limited conditions (C2), wells show strong and increasing downward trends: 20% over 19 years and 29% over 9 years, far exceeding upward trends. In contrast, wells in flat-gradient areas (C1 and C3) show little change in trend activity between the 19-year and 9-year periods. However, because small shifts can trigger SWI, we used 9-year GWL trends to project which areas may enter, remain in, or exit SWI-susceptible conditions over the next decade (Fig. 3B). Persistent gradient-based hotspots (92.0% of all sites that are currently and/or projected to be in C1 or C3) are locations already exhibiting SWI-susceptible conditions that are projected to remain within C1 or C3 over the next decade. A smaller fraction (3.7%) are projected to stabilize, meaning they may transition out of C1/C3 classification if recent upward trends continue, and 4.3% are emerging hotspots.

Regions showing the highest share of significant downward GWL changes over the 9-year period include western South Africa (WSAF), India (SAS), southeastern Australia (EAU), western North America (WNA), Mexico (NCA and SCA), and southern Europe (MED) (Fig. 2). Some of these regions display similar patterns over the 19-year period, while others (such as SAS and EAU) show a shift toward more upward or balanced GWL changes (Supplement B-3). In contrast, areas such as central North America (CNA), northern Brazil (NES), and northern Australia (NAU) show more frequent upward or balanced trend

directions. Northern and western central Europe (NEU, WCE) exhibit relatively low trend activity, with fewer than 10 % of observations showing significant GWL changes in either direction. Meanwhile, Fig. 3B shows projected changes in flat-gradient conditions, alongside their current distribution. Some regions with predominantly declining GWLs, such as South Africa, generally have steeper gradients, whereas flat gradients are common elsewhere. Emerging and stabilizing hotspots mainly occur, and tend to cluster within subregions, where downward and upward GWL changes were observed, respectively (compare Fig. 2). Declining GWLs have an especially pronounced influence on the development of flat-gradient conditions in eastern Australia (EAU).

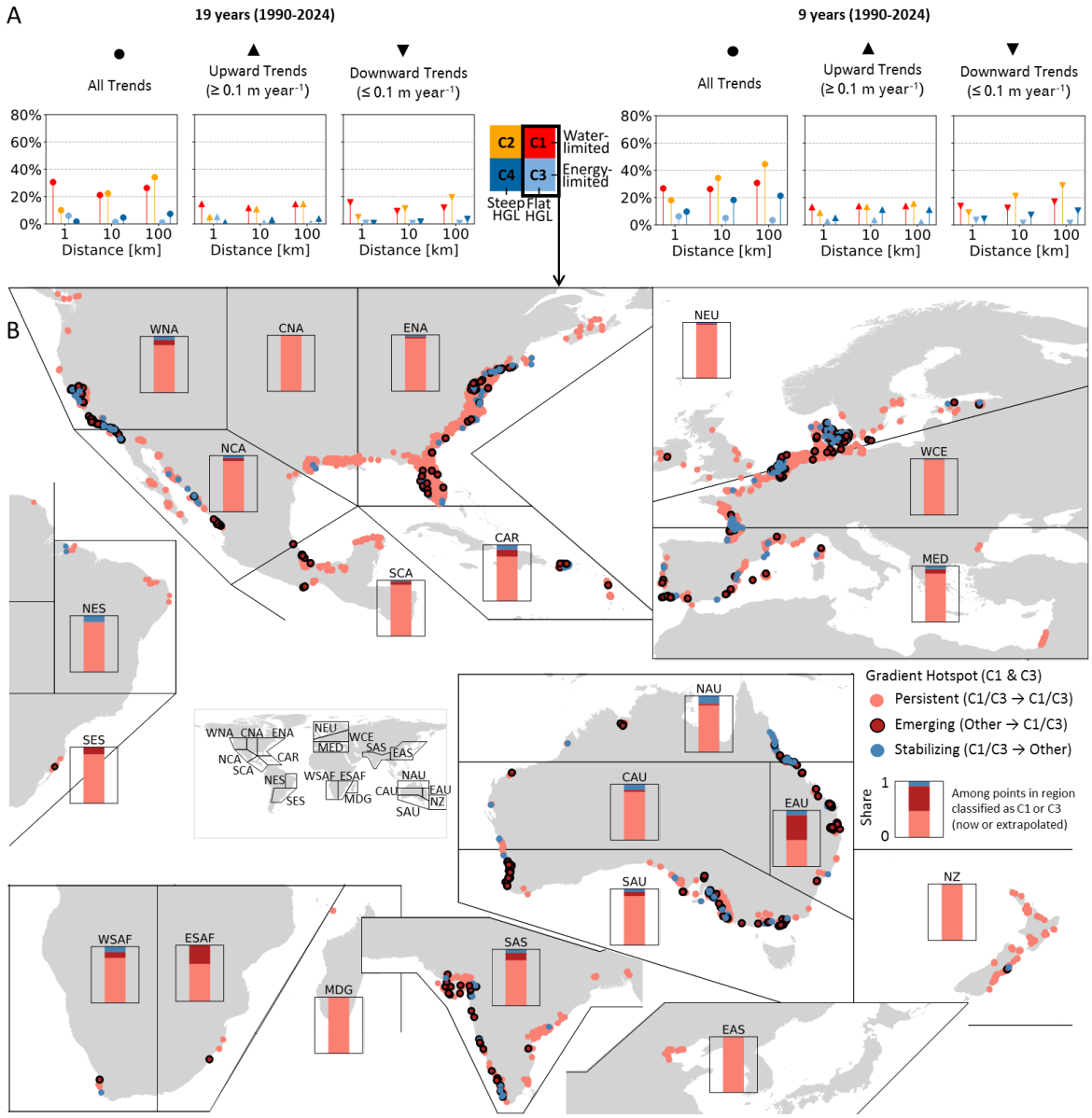

Fig. 3 (A) Proportion of groundwater trends over 19 and 9 years assigned into susceptibility clusters C1–C4. Columns separate trend directions: all trends, increasing (≥ 0.1 m year^{-1}), and decreasing (≤ –

0.1 m year^{-1}), across three coastal distance bins (1, 10, and 100 km). Bars are color-coded by cluster. (B) Spatial patterns of hydroclimatic gradient-based groundwater susceptibility hotspots across IPCC-defined subregions (Iturbide *et al* 2020), derived from 9-year trend extrapolation and susceptibility classification. Colored points represent individual observations, plotted in grid cell centers; emerging and stabilizing hotspots are randomly overlaid on persistent hotspots when co-located. Hotspot types include: persistent (C1/C3 now and in 10 years), emerging (not currently C1/C3, but extrapolated to enter within 10 years), stabilizing (currently C1/C3, extrapolated to exit within 10 years). Bar charts show the relative proportions of projected hotspot status (persistent, emerging, stabilizing) among all observations within each region that are either currently, or projected to be, classified as C1 or C3.

Discussion

The results of this study confirm and extend previous findings by integrating in-situ GWL observations with physically relevant indicators across an unprecedentedly large and diverse set of coastal areas. Building on the elevation-based susceptibility framework applied by Jasechko *et al* (2020), which identified U.S. coastal areas with GWLs below sea level as potential SWI hotspots, we applied a related but expanded approach that incorporates groundwater hydraulic gradients based on an established threshold (≤0.001; Ferguson and Gleeson 2012, Kretschmer *et al* 2025a), and hydroclimatic conditions. Regions along the U.S. coasts that we identified as hydroclimatically susceptible show strong spatial concordance with areas highlighted by Jasechko *et al* (2020). For example, our results show that 20% of CGWL observations within 10 km of the U.S. coastline exhibit GWLs below sea level, broadly consistent with the 27% of individual wells reported by Jasechko *et al* (2020) for the same distance. In addition, the spatial overlap between our hydroclimatically susceptible regions and documented SWI cases compiled by Cao *et al* (2021) and Kretschmer *et al* (2025b) (Fig. 3 and Fig. 1 in respective papers) supports the relevance of our framework. Many areas classified as flat-gradient and arid (C1) in our analysis correspond to previously reported SWI sites, including the southeastern and Gulf coasts of the U.S., the Mediterranean, Cape Town, India, and eastern Australia.

The GWL trend analysis adds a dynamic dimension to previously static susceptibility assessments. We found signals of GWL declines that reinforce their susceptibility status, e.g., the southeastern U.S., Gulf Coast, and Florida, as well as southwestern India, parts of the European Mediterranean, and southeastern and southern Australia. In many of these areas, recent declines are sufficient to push aquifers across the hydraulic gradient threshold that defines heightened susceptibility, and fewer sites show recovery strong enough to exit those conditions within the next decade. Even small deviations from this threshold can be critical in the face of rising seas, with the current global mean sea-level rise rate of ~4.5 mm year^{-1} (Hamlington *et al* 2024).

Notably, the spatial distribution of significant GWL changes does not align with population density. Rural coastal areas show both a higher frequency and magnitude of GWL trends than urban areas. While these trends are only dominantly downward in some regions, our results align with Jasechko *et al* (2024), who

found widespread declines in dryland aquifers, particularly under croplands. Hence, there might be a disproportionate SWI susceptibility of groundwater-dependent agricultural regions, where high extraction pressures coincide with limited regulatory oversight (consistent with global, sector-resolved withdrawal trends indicating agriculture as the dominant groundwater user and increasing withdrawals in many regions since 2001; Nazari *et al* 2025). Our results also show that rising GWLs are as frequent as declining ones, both globally and often regionally. These upward trends may reflect recovery, climate variability, or management interventions. Especially regions with spatio-temporal inconsistent trends require careful interpretation and hence data support. The comparison of 9- and 19-year trends adds temporal nuance to trend analysis. While Chávez García Silva *et al* (2024) reported largely stable long-term GWLs across southwestern Europe (1980–2020), our shorter-term results reveal more spatially variable coastal patterns, including more frequent and stronger declines in more recent years. On the one hand, recent changes may be masked in longer-term regional assessments. On the other hand, long-term records help reduce misinterpretation driven by short-term variability or episodic recovery. Another example is modest declines over 19 years, but consistent downward trends over the past 9 years we found in India.

It is important to acknowledge limitations in our data-driven groundwater assessments. In addition to the uncertainties in the groundwater dataset and trend calculations (mainly discussed in the Supplements), some limitations come with our approach of relating these observations to SWI susceptibility. Our approach necessarily simplifies the physical complexity of coastal aquifer systems, where salinization can propagate through multiple interconnected pathways: over land (storm surge and tidal flooding), under land via groundwater transport, and through natural and engineered surface-water networks (Helton *et al* 2025). The conceptual thresholds we applied (shallow WTD, low hydraulic gradients, and water-limited (arid) conditions) function as first-order proxies for SWI susceptibility but do not capture processes such as density-driven flow, tidal dynamics, and transient interface responses (Shamsudduha *et al* 2009, Werner *et al* 2012). Gradient-based risk estimates assume fresh groundwater, as salinity data are largely unavailable. The aridity index offers a practical proxy for recharge limitation, but its categorical application may obscure climatic seasonality and group ecologically distinct regions (Taylor *et al* 2013, Trabucco and Zomer 2018).

Our dataset directly addresses the urban bias noted by Kretschmer *et al* (2025b), who found that coastal groundwater studies are disproportionately located in urban, economically developed regions. Nevertheless, limited data coverage in many coastal regions constrains the global validity of our results. There is a geographic bias in data coverage toward temperate regions such as Europe and the United States, and several SWI sites in the literature in Asia, Africa, and South America (Cao *et al* 2021, Kretschmer *et al* 2025a) fall outside of our studied regions. Our use of grid-based aggregation helps harmonize comparisons across regions with uneven well densities, but may obscure localized heterogeneity caused by pumping, aquifer

layering, or confined conditions. As such, while our framework offers a valuable screening tool for identifying potentially susceptible coastal settings, finer-scale vulnerability assessments will require more detailed hydrogeologic characterization, higher-resolution elevation and well metadata, and more systematic treatment of anthropogenic influences and observational uncertainty.

Conclusions

This study presents the first global assessment of coastal groundwater systems based on in-situ GWL observations. It provides data-informed insight into where and how coastal aquifers are already exhibiting signs of increased susceptibility to SWI. Our approach captures spatiotemporal signals that are often overlooked by global models or static frameworks. The analysis shows that coastal aquifers are not merely facing SWI in theory, but in many cases are already experiencing or crossing thresholds that signal increased susceptibility.

One of the clearest signals emerges near the coast. Within 1 km of the coastline, nearly one-third of all sites falling into the most susceptible hydroclimatic conditions (flat groundwater gradients combined with arid climates) show significant GWL trends, indicating ongoing system transitions in zones that are physically least buffered against SWI. Notably, these trends occur in both upward and downward directions, suggesting that coastal systems are responding dynamically to climate variability, land use, and water management. In parallel, our findings reveal a growing disconnect between where GWL changes are occurring and where monitoring and management are focused. Rural and inland coastal zones show a consistently higher prevalence of significant GWL trends compared to urban areas, yet remain underrepresented in both data coverage and risk assessments. At the same time, regions such as India, southeastern Australia, the Mediterranean, Mexico, and different parts of the United States combine physical susceptibility with pronounced GWL changes (including more pronounced declines in recent years), while areas like western South Africa show strong declines but with less consistent physical susceptibility. These regions should be prioritized for observation, intervention, and targeted data synthesis, such as joint analyses with sector-resolved withdrawal datasets.

Our trend extrapolation further shows that nearly all sites currently exhibiting flat gradients and either arid or low-recharge conditions are projected to remain susceptible over the next decade if recent GWL changes continue. Additional sites are likely to transition into these high-risk states, pointing to the continued expansion of SWI-relevant risk zones in the near future. These findings underscore the importance of shifting from static toward dynamic, observation-driven susceptibility tracking. Many coastal zones are entering susceptibility states in real time, yet management approaches that assume long-term stability or rely solely on elevation-based proxies, such as equilibrium model outputs, might underestimate current

exposure. GWL time series must be systematically incorporated into SWI risk assessments, and global models should include observational constraints. We therefore highlight the urgency of improving data infrastructure, especially since significant data gaps persist across equatorial regions, much of Africa, and large parts of Asia.

Methods

We used the Coastal Groundwater Level (CGWL) dataset, a global compilation of over 550,000 in-situ GWL time series obtained from governmental monitoring networks and public portals (see Supplement A). Raw groundwater data were selected and standardized following consistent criteria, and gridded groundwater depth and groundwater elevation estimates were generated. Together, the gridded dataset and the GWL time series form the basis for all spatiotemporal analyses in this study. We refer to individual entries in the gridded dataset as observations. These refer to in-situ-based aggregates at the grid-cell level, not the original point-level measurements.

Groundwater gradient and trend analysis

Spatiotemporal groundwater patterns were assessed through two key variables: hydraulic gradients and GWL trends. Hydraulic gradients were calculated at the grid level as the ratio between the median groundwater elevation (aggregated from wells within each grid cell) to the median Euclidian distance to the coastline of all wells in that cell. We acknowledge sources of uncertainty in the value estimates of both input parameters and gridding (see Supplement A for more details) and that hydraulic gradients are inherently dynamic and influenced by local hydrogeologic complexity. However, in the absence of consistent, high-resolution global data on aquifer characteristics, this approach provides a simplified yet scalable approximation of prevailing gradient conditions. The sample size for hydraulic gradient analysis comprised 232,419 grid cells with available groundwater elevation and coastline distance data.

To assess recent trends in coastal GWLs, we selected time series spanning the past available 9 and 19 years between 1990 and 2024. These thresholds were based on data availability, determined iteratively to balance temporal and spatial coverage across the global dataset. The 19-year window provides a more robust estimate of long-term changes, especially in aquifers with low-frequency variability or delayed responses to climate and land surface conditions, which can span years to decades depending on hydrogeologic setting (Cuthbert *et al* 2019a, Baulon *et al* 2022). The 9-year trends may reflect more recent or emerging shifts in coastal groundwater systems, similar to the ~10-year observation window used in Jasechko *et al* (2024). The longest valid time series segment per well was selected. If it spanned 19 years, the 9-year trend was derived from its final 9 years; otherwise, only a chosen 9-year trend was calculated. A total of 51,263 (9-

year) and 20,857 (19-year) trends were calculated from unique well locations. Time series for trends were selected based on criteria for temporal completeness and minimum data continuity. Monotonic trends in GWLs were calculated using the non-parametric modified Mann-Kendall test (Yue and Wang 2004), and corresponding trend magnitudes were estimated using Sen's slope (Sen 1968). Further details on the time series selection and filtering criteria for trend analysis are provided in Supplement B-1. Due to the prevalence of short and seasonally biased records, particularly in global datasets, trend interpretations are subject to uncertainty. While longer time series better capture low-frequency variability and reduce the influence of short-term fluctuations, inconsistencies in trends across time windows or nearby wells are common in groundwater systems and reflect both data limitations and complex hydroclimatic and anthropogenic interactions (further discussed in Supplement B-2).

Trends and trend consistency were computed at the well level and subsequently aggregated to grid cells by taking the median of slope values, regardless of individual statistical significance; however, significance flags were retained to support additional filtering. Trend slopes were classified into five trend categories: strongly downward (< -0.5 m $year^{-1}$), moderately downward (-0.5 to -0.1 m $year^{-1}$), no trend (between -0.1 and 0.1 m $year^{-1}$ and/or non-significant), moderately upward (0.1 to 0.5 m $year^{-1}$), and strongly upward (> 0.5 m $year^{-1}$). Only a small fraction of results classified as "no trend" are non-significant solely due to statistical insignificance (5.6% for 9-year trends and 1.7% for 19-year trends).

Hydroclimatic classification

The conceptual hydroclimatic susceptibility space introduced in this study was operationalized along three axes: aridity (as a proxy for water availability), water table depth (as a measure of buffering capacity), and hydraulic gradient (which determines the system's ability to maintain seaward freshwater flow). Regions that are both water-limited and hydraulically flat represent configuration of elevated susceptibility to SWI, particularly if groundwater is shallow. To classify hydraulic gradients, we used two categories based on model-informed thresholds: flat (< 0.001) and steep (> 0.001), following Ferguson and Gleeson (2012) and Kretschmer *et al* (2025a), who showed that gradients below 0.001 are more prone to SWI or to the persistence of saline groundwater. Each grid cell was further assigned an aridity index (AI) from Zomer *et al* (2022), which represents the ratio of precipitation to potential evapotranspiration and reflects recharge limitation. Cells were categorized as either water-limited ($AI \leq 1$) or energy-limited ($AI > 1$).

By combining this climate classification with in-situ groundwater observations, the analysis provides a first-order, observation-informed perspective on physical configurations under which coastal aquifers may exhibit increased susceptibility to SWI. Hydraulic gradient and aridity categories were then combined to define four hydroclimatic clusters:

- C1 (most susceptible): Flat gradient (≤ 0.001) & water-limited (AI ≤ 1)
- C2: Steep gradient (> 0.001) & water-limited
- C3: Flat gradient & energy-limited (AI > 1)
- C4 (least susceptible): Steep gradient & energy-limited

These clusters form the basis for comparing hydroclimatic susceptibility patterns across global coastal regions. To identify potential current and future hotspots of SWI susceptibility, we focused on areas with flat hydraulic gradients. Using recent 9-year GWL trend slopes, we extrapolated values over a 10-year horizon to assess whether such continued changes would cause grid cells to shift into or out of hydroclimatic susceptibility clusters C1 (flat & water-limited) and C3 (flat & energy-limited). This provides a first-order approximation of where continued trends may trigger SWI-relevant conditions, recognizing that such projections do not account for potential nonlinearities or management responses.

Acknowledgments

The authors would like to thank all of the governmental agencies listed in Supplement A that supported this work by providing groundwater data and being available to answer questions about the data.

CRediT authorship contribution statement

A. Nolte: Conceptualization, Data curation, Formal analysis, Investigation, Methodology, Writing – original draft, Writing – review & editing. **S. Bender:** Funding acquisition, Supervision, Writing – review & editing. **J. Hartmann:** Funding acquisition, Supervision, Writing – review & editing. **S. Baltruschat:** Writing – review & editing. **N. Moosdorf:** Methodology, Writing – review & editing. **R. Reinecke:** Conceptualization, Formal analysis, Methodology, Writing – original draft, Writing – review & editing

Data availability statement

The CGWL dataset is publicly available on Zenodo under a CC-BY-NC license, including all data sources obtained with permission for publishing or under open licenses: [link will be provided in peer-reviewed manuscript]. Code and data for conducting trend and SWI susceptibility analyses are also available on Zenodo: [link will be provided in peer-reviewed manuscript]. Additional datasets used in these analyses are referenced within the same repository.

References

Adams K H, Reager J T, Buzzanga B A, David C H, Sawyer A H and Hamlington B D 2024 Climate-Induced Saltwater Intrusion in 2100: Recharge-Driven Severity, Sea Level-Driven Prevalence *Geophys Res Lett* **51** e2024GL110359

Baulon L, Allier D, Massei N, Bessiere H, Fournier M and Bault V 2022 Influence of low-frequency variability on groundwater level trends *J. Hydrol.* **606** 127436

Berghuijs W R, Collenteur R A, Jasechko S, Jaramillo F, Luijendijk E, Moeck C, van der Velde Y and Allen S T 2024 Groundwater recharge is sensitive to changing long-term aridity *Nat. Clim. Chang.* **14** 357–63

Cao T, Han D and Song X 2021 Past, present, and future of global seawater intrusion research: A bibliometric analysis *J. Hydrol.* **603** 126844

Chávez García Silva R, Reinecke R, Copty N K, Barry D A, Heggy E, Labat D, Roggero P P, Borchardt D, Rode M and Gómez-Hernández J J 2024 Multi-decadal groundwater observations reveal surprisingly stable levels in southwestern Europe *Communications Earth & Environment* **5** 387

CIESIN 2018 Gridded Population of the World, Version 4 (GPWv4): Population Density, Revision 11, NASA Socioeconomic Data and Applications Center (SEDAC) [dataset]

Cosby A G, Lebakula V, Smith C N, Wanik D W, Bergene K, an Rose, Swanson D and de Bloom 2024 Accelerating growth of human coastal populations at the global and continent levels: 2000–2018 *Scientific reports* **14** 22489

Costall A R, Harris B D, Teo B, Schaa R, Wagner F M and Pigois J P 2020 Groundwater Throughflow and Seawater Intrusion in High Quality Coastal Aquifers *Sci. Reports* **10** 9866

Costantini M, Colin J and Decharme B 2023 Projected Climate-Driven Changes of Water Table Depth in the World's Major Groundwater Basins *Earth's Future* **11**

Cuthbert M O, Gleeson T, Moosdorf N, Befus K M, Schneider A, Hartmann J and Lehner B 2019a Global patterns and dynamics of climate–groundwater interactions *Nat. Clim. Chang.* **9** 137–41

Cuthbert M O, Taylor R G, Favreau G, Todd M C, Shamsudduha M, Villholth K G, MacDonald A M, Scanlon B R, Kotchoni D V and Vouillamoz J-M 2019b Observed controls on resilience of groundwater to climate variability in sub-Saharan Africa *Nature* **572** 230–4

Dyring M, Hofmann H, Stanton D, Moss P and Froend R 2022 Ecohydrology of coastal aquifers in humid environments and implications of a drying climate *Ecohydrology*

Eurostat 2021 *Applying the Degree of Urbanisation. A Methodological Manual to Define Cities, Towns and Rural Areas for International Comparisons* (Luxembourg: European Union/FAO/UN-Habitat/)

Famiglietti J S and Rodell M 2013 Water in the Balance *Science (New York, N.Y.)* **340** 1299–300

Fan X, Peterson T J, Henley B J and Arora M 2023 Groundwater sensitivity to climate variations across Australia *Water Res* **59** e2023WR035036

Fan Y, Li H and Miguez-Macho G 2013 Global patterns of groundwater table depth *Science* **339** 940–3

Ferguson G and Gleeson T 2012 Vulnerability of coastal aquifers to groundwater use and climate change *Nat. Clim. Change* **2** 342–5

Frappart F and Ramillien G 2018 Monitoring Groundwater Storage Changes Using the Gravity Recovery and Climate Experiment (GRACE) Satellite Mission: A Review *Remote Sens.* **10** 829

Gleeson T *et al* 2021 GMD perspective: The quest to improve the evaluation of groundwater representation in continental- to global-scale models *Geosci. Model Dev.* **14** 7545–71

Gleeson T, Cuthbert M, Ferguson G and Perrone D 2020 Global Groundwater Sustainability, Resources, and Systems in the Anthropocene *Annu. Rev. Earth Planet. Sci.* **48** 431–63

Hamlington B D, Bellas-Manley A, Willis J K, Fournier S, Vinogradova N, Nerem R S, Piecuch C G, Thompson P R and Kopp R 2024 The rate of global sea level rise doubled during the past three decades *Communications Earth & Environment* **5** 601

Helton A M, Dennedy-Frank P J, Emanuel R E, Neubauer S C, Adams K H, Ardon M, Band L, Befus K M, Borstlap H and Duberstein J A 2025 Over, under, and through: Hydrologic connectivity and the future of coastal landscape salinization *Water Res* **61** e2024WR038720

IPCC 2021 Climate change 2021: The Physical Science Basis: Contribution of Working Group I to the Sixth Assessment Report of the Intergovernmental Panel on Climate Change 2391

Iturbide M *et al* 2020 An update of IPCC climate reference regions for subcontinental analysis of climate model data: definition and aggregated datasets *Earth Syst. Sci. Data* **12** 2959–70

Jasechko S, Perrone D, Seybold H, Fan Y and Kirchner J W 2020 Groundwater level observations in 250,000 coastal US wells reveal scope of potential seawater intrusion *Nature communications* **11** 3229

Jasechko S, Seybold H, Perrone D, Fan Y, Shamsudduha M, Taylor R G, Fallatah O and Kirchner J W 2024 Rapid groundwater decline and some cases of recovery in aquifers globally *Nature* **625** 715–21

Kretschmer D V, Michael H, Moosdorf N, Essink G O, Bierkens M F P, Wagener T and Reinecke R 2025a Controls on coastal saline groundwater across North America *Environ. Res. Lett.*

Kretschmer D V, Michael H A, Moosdorf N, Oude Essink G H P, Bierkens M F P, Wagener T and Reinecke R 2025b A Perceptual Model of Drivers and Limiters of Coastal Groundwater Dynamics *Hydrol. Process.* **39** e70058

Lall U, Josset L and Russo T 2020 A Snapshot of the World's Groundwater Challenges *Annu. Rev. Environ. Resour.* **45** 171–94

Ma Y, Leonarduzzi E, Defnet A, Melchior P, Condon L E and Maxwell R M 2024 Water table depth estimates over the contiguous united states using a random forest model *Groundwater* **62** 34–43

Michael H A, Russoniello C J and Byron L A 2013 Global assessment of vulnerability to sea-level rise in topography-limited and recharge-limited coastal groundwater systems *Water Resour. Res.* **49** 2228–40

Morgan L K and Werner A D 2015 A national inventory of seawater intrusion vulnerability for Australia *Journal of Hydrology: Regional Studies* **4** 686–98

Nazari S, Reinecke R and Moosdorf N 2025 Global estimates of groundwater withdrawal trends and uncertainties *Environ. Res. Lett.*

Neumann B, Vafeidis A T, Zimmermann J and Nicholls R J 2015 Future coastal population growth and exposure to sea-level rise and coastal flooding-a global assessment *PloS one* **10**

Reinecke R, Gnann S, Stein L, Bierkens M, Graaf I de, Gleeson T, Essink G O, Sutanudjaja E H, Vargas C R and Verkaik J 2024 Uncertainty in model estimates of global groundwater depth *Environ. Res. Lett.* **19** 114066

Renu S, Pramada S K and Yadav B K 2025 Seawater intrusion susceptibility and modeling: A case study of Kerala, India *Acta Geophysica* **73** 1927–45

Richardson C M, Davis K L, Ruiz-González C, Guimond J A, Michael H A, Paldor A, Moosdorf N and Paytan A 2024 The impacts of climate change on coastal groundwater *Nature Reviews Earth & Environment* 1–20

Sen P K 1968 Estimates of the regression coefficient based on Kendall's tau *Journal of the American statistical association* **63** 1379–89

Shamsudduha M, Chandler R E, Taylor R G and Ahmed K M 2009 Recent trends in groundwater levels in a highly seasonal hydrological system: the Ganges-Brahmaputra-Meghna Delta *Hydrol. Earth Syst. Sci.* **13** 2373–85

Shokri-Kuehni S M S, Raaijmakers B, Kurz T, Or D, Helmig R and Shokri N 2020 Water table depth and soil salinization: From pore-scale processes to field-scale responses *Water Res* **56** e2019WR026707

Spinoni J, Barbosa P, Cherlet M, Forzieri G, McCormick N, Naumann G, Vogt J V and Dosio A 2021 How will the progressive global increase of arid areas affect population and land-use in the 21st century? *Global and Planetary Change* **205** 103597

Taylor R G, Scanlon B, Döll P, Rodell M, van Beek R, Wada Y, Longuevergne L, Leblanc M, Famiglietti J S and Edmunds M 2013 Ground water and climate change *Nat. Clim. Chang.* **3** 322–9

Trabucco A and Zomer R 2018 Global Aridity Index and Potential Evapotranspiration (ET0) Climate Database v2 *CGIAR Consort Spat Inf* **10**

United Nations 2022 The United Nations World Water Development Report 2022: Groundwater - Making the invisible visible

Werner A D, Ward J D, Morgan L K, Simmons C T, Robinson N I and Teubner M D 2012 Vulnerability indicators of sea water intrusion *Groundwater* **50** 48–58

Yue S and Wang C 2004 The Mann-Kendall test modified by effective sample size to detect trend in serially correlated hydrological series *Water Resour Manage* **18** 201–18

Zamrsky D, Oude Essink G H P and Bierkens M F P 2024 Global impact of sea level rise on coastal fresh groundwater resources *Earth's Future* **12** e2023EF003581

Zomer R J, Xu J and Trabucco A 2022 Version 3 of the global aridity index and potential evapotranspiration database *Scientific data* **9** 409